REPORT DOCUMENTATION PAGE

Form Approved
OMB No. 0704-0188

1. REPORT DATE (DD-MM-YYYY)	2. REPORT TYPE Technical Papers	3. DATES COVERED (From - To)

4. TITLE AND SUBTITLE	5a. CONTRACT NUMBER
	5b. GRANT NUMBER
	5c. PROGRAM ELEMENT NUMBER

6. AUTHOR(S)	5d. PROJECT NUMBER 2362
	5e. TASK NUMBER MIG2
	5f. WORK UNIT NUMBER

7. PERFORMING ORGANIZATION NAME(S) AND ADDRESS(ES)	8. PERFORMING ORGANIZATION REPORT
Air Force Research Laboratory (AFMC) AFRL/PRS 5 Pollux Drive Edwards AFB CA 93524-7048	

9. SPONSORING / MONITORING AGENCY NAME(S) AND ADDRESS(ES)	10. SPONSOR/MONITOR'S ACRONYM(S)
Air Force Research Laboratory (AFMC) AFRL/PRS 5 Pollux Drive Edwards AFB CA 93524-7048	11. SPONSOR/MONITOR'S NUMBER(S)

12. DISTRIBUTION / AVAILABILITY STATEMENT

Approved for public release; distribution unlimited.

13. SUPPLEMENTARY NOTES

14. ABSTRACT

15. SUBJECT TERMS

16. SECURITY CLASSIFICATION OF:			17. LIMITATION OF ABSTRACT	18. NUMBER OF PAGES	19a. NAME OF RESPONSIBLE PERSON Leilani Richardson
a. REPORT Unclassified	b. ABSTRACT Unclassified	c. THIS PAGE Unclassified	A		19b. TELEPHONE NUMBER (include area code) (661) 275-5015

36 separate flies are enclosed

MEMORANDUM FOR PR (Contractor/In-House Publication)

FROM: PROI (TI) (STINFO)   17 Apr 2000

SUBJECT: Authorization for Release of Technical Information, Control Number: **AFRL-PR-ED-TP-2000-067**
Smith, C.W. & Gloss, K.T (Virginia Polytechnic Institute and State University), Constantinescu, D.M.
(Bucharest Polytechnic University), and Liu, C.T., "Stress Intensity Factors for Cracks Within and Near to
Bondlines in Soft Incompressible Materials"

2000ASME International Mechanical Engineering Congress   **(Statement A)**
(Orlando, FL 05-10 Nov 2000) (Submission Deadline: 28 April 2000)

1. This request has been reviewed by the Foreign Disclosure Office for: a.) appropriateness of distribution statement,
b.) military/national critical technology, c.) export controls or distribution restrictions,
d.) appropriateness for release to a foreign nation, and e.) technical sensitivity and/or economic sensitivity.
Comments:_____
_____
_____
_____

Signature _____   Date _____

2. This request has been reviewed by the Public Affairs Office for: a.) appropriateness for public release
and/or b) possible higher headquarters review.
Comments: _____
_____
_____
_____

Signature _____   Date _____

3. This request has been reviewed by the STINFO for: a.) changes if approved as amended,
b.) appropriateness of distribution statement, c.) military/national critical technology, d.) economic sensitivity,
e.) parallel review completed if required, and f.) format and completion of meeting clearance form if required
Comments:_____
_____
_____

Signature _____   Date _____

4. This request has been reviewed by PR for: a.) technical accuracy, b.) appropriateness for audience, c.)
appropriateness of distribution statement, d.) technical sensitivity and economic sensitivity, e.) military/
national critical technology, and f.) data rights and patentability
Comments:_____
_____

                              APPROVED/APPROVED AS AMENDED/DISAPPROVED

                              _____
                              ROBERT C. CORLEY   (Date)
                              Senior Scientist (Propulsion)
                              Propulsion Directorate

20021119 111

STRESS INTENSITY FACTORS FOR CRACKS WITHIN AND NEAR TO BONDLINES IN SOFT INCOMPRESSIBLE MATERIALS

C. W. Smith*, K. T. Gloss*,
D. M. Constantinescu † and C. T. Liu‡

* Department of Engineering Science and Mechanics
Virginia Polytechnic Institute and State University
Blacksburg, VA 24061

† On Sabbatical from Bucharest Polytechnic University

‡ Air Force Research Laboratory, PRSM
10 E. Saturn Blvd.
Edwards, AFB, CA 93524-7680

ABSTRACT

Using a polyurethane photoelastic material, thick test specimens of several configurations with bonded end tabs are examined for measuring stress intensity factors (SIFs) for cracks within and near to bondlines in bonded photoelastic models. Effects of specimen height, glued end tabs, bondline and crack size and location are studied and analyzed using a two parameter model for extracting the SIFs and results are compared with cracked, homogeneous model results.

INTRODUCTION

Large volumes of particulate composites are finding use in many applications in the commercial and military transportation industry. One of these is solid propellant, which consists of hard polyhedral particles embedded in a soft rubber matrix which stiffens at low temperatures. The presence of defects, mainly cracks, in structures composed of these materials has become important as a result of efforts to extend the life of these structures for economic reasons.

When a crack occurs in such a structure during storage or transport, it may extend under a given or changing environment until it becomes sufficiently large to affect the structural and operational integrity of the unit. When a crack grows in such a material, the matrix ahead of the crack tip stretches, separating into strands and producing severe blunting and moving the hard particles above and below the crack plane until the crack breaks the strands to advance through the stretch zone. This blunt-growth-process is repeated, producing a highly non-linear phenomena. At very low temperatures, the stretching of the matrix is suppressed, producing an embrittling effect.

In order to bypass the complications described above, designers often treat the composite as a homogeneous material using average properties. In establishing average properties for cracks in soft bonded structures, glued end tabs must be used with relatively simple test geometries. The present study uses this approach in order to measure effects of specimen geometry, end tabs, crack location and bondlines on the stress intensity factors for cracks within and near to the bondlines and compares results with unbonded specimen results.

1

THE EXPERIMENTAL METHOD

The photoelastic method was used to analyze all specimens. The method uses stress fringe patterns obtained from tension tests of photoelastic models. The fringes are loci of constant maximum shear stress magnitude. In order to convert the test data into fracture parameters, in this case stress intensity factors, (SIF^s), it is necessary to have an algorithm for this conversion. The authors used a two parameter algorithm developed some time ago (Smith and Kobayashi, 1993) for homogeneous materials. This method is valid in this work since the interface fracture equations (Hutchinson and Suo, 1992) reduce to homogeneous form for bondline cracks in thick, incompressible bodies. The algorithm for Mode I loading is briefly described in the Appendix.

THE EXPERIMENTS

The experiments can be divided into two basic categories:

1. Bonded specimens containing double edge bondline cracks and

2. Bonded specimens with single edge cracks near to and parallel to the bondline.

1. <u>Bondline Cracks</u>

A series of polyurethane test specimens (Fig. 1) was prepared with double edge cracks in the bondline for both square specimens and some with the specimen height reduced by half. Specimen ends were inserted into grooves in aluminum plates and bonded to simulate methods used for bonding solid propellant material specimens. The extent to which this method achieves a uniform axial stress field in the direction

of the load will be shown by global stress fringe photographs of the test specimens under load. The analytical models also assume zero transverse displacement of the test specimen at the boundaries. Companion tests were run for different crack lengths. These specimens were made by fitting the adherends to teflon coated razor blades on each side of the specimen and then pouring an adhesive with a modules higher than the polyurethane adherends into the opening in between and then curing at 160°F for 12 hrs., after which the razor blades were removed. It has been previously found (Smith, Finlayson and Liu, 1998) that modulus mismatch between adherends exerted negligible effect upon the SIF values for the cracks within the bondline for modulus ratios not exceeding about 3.5 so no modulus mismatch was introduced into the models.

Figs. 2a and 2b are global fringe photos from a parallel circular polariscope using monochromatic light of the square and short specimens respectively under load. They reveal some irregularities along the fixed edges possibly due to adhesive slippage. This results in slight dysymmetry of the near tip fringe patterns but the effect on K_1 is well within the expected experimental scatter of ±5%. This effect was accommodated by averaging the K_1 values for the two cracks in each specimen. Figs 3a and 3b show that the near tip fringe patterns show no rotation of the fringe loops which suggest the absence of any shear mode K_2. The data zones for K_1 determination in Figure 3 are taken along a line normal to the crack plane and passing through the tip of the crack. The data zone locations are indicated. The dark bands surrounding the crack opening in Fig. 3 are part of the crack surface which turns outward due to increased crack opening at

the near surface of the specimen.

2. Cracks Parallel to the Bondline

In this experimental study, a series of photoelastic experiments were conducted on bonded plates consisting of small cracks of various lengths parallel to the bondline between adherends of the same modulus bonded with an adhesive of somewhat higher modulus to effect a fairly strong bond. Both square and rectangular specimens were analyzed, the latter consisting of heights of half of the square specimens as above.

The studies were conducted under dead weight loading with uniform displacements along the edge of the grips. The specimens were glued to slots in aluminum grips without additional restraints in order to study such a gripping arrangement.

A typical specimen is pictured in Fig. 4. After machining and bonding the adherends, the crack was introduced by using a small saw with a razor blade as the cutting edge. After inserting into aluminum grips and bonding to them, the specimens were dead loaded, with the load on the lower grip being adjusted to keep the lower grip perfectly horizontal. Tests comparing a clamped upper grip with the pin hole arrangement yielded identical results so the pin hole arrangement at the upper grip was used. Room temperature values of modulus were measured to be 4.7 MPa and the value of Poisson's Ratio was 0.50. The nominal value of the adhesive modulus was given by the manufacturer to be 6.9 MPa.

The specimens were loaded and photographed in a crossed circular polariscope using monochromatic light. The near tip fringe patterns were analyzed using the two parameter method described in the Appendix.

Typical global and local photographs were shown in Fig. 5, for a square specimen (SP11). The global fringe pattern (Fig. 5a) suggests some local slippage near the center of the specimen in the upper grips and an unsymmetric pattern near the lower grips due to the crack. The local fringe pattern (Fig. 5b) clearly reveals a pure Mode 1 pattern near the crack tip (i.e. no rotation of the near tip fringe loops) but a clear presence (i.e. loop folding into a butterfly shape) of the non-singular stress parallel to the crack.

Zones from which test data for computing the SIF values were taken are indicated in (Fig. 5b). SIF values were determined both above and below the crack tip and averaged to minimize error due to the crack tip location, and then normalized with respect to $K_0 = \bar{\sigma}(\pi a)^{1/2}$ where $\bar{\sigma}$ was the remote average stress.

In these thick plate experiments, for both bondline cracks and those parallel to the bondline, some transverse constraints, tip blunting, and edge curling along the upper and lower crack surfaces occurred, so a single edge crack photoelastic test on a homogeneous thick plate was run and the results compared with an accurate two dimensional solution (Gross, Srawley and Brown, 1964) obtained by boundary collocation. This comparison suggested that the test results were 7.8% higher than predicted and this factor was used to correct all of the test data for the above noted three dimensional effects. The effect of the bondline was to constrict the size of the data zone between the bondline and the crack tip (Fig. 5b) which also altered the value of the nonsingular stress σ_{ij}^0 but not the value of K_1.

3

RESULTS

1) Bondline cracks

Using the near tip fringe pattern photos, the algorithm described in the Appendix was used to extract K_1 values from the local fringe pattern data. An example of the procedure is given in Fig. A-2. K_1 values were computed both above and below the bondline and agreed to well within experimental scatter of 5%. A summary of the test data and results are found in Table 1.

A plot of the results for the square and short specimen test data are presented in Fig. 6. Also shown is the theoretical solution for the double edge crack with no bondline due to Bowie (1964). The experimental data are corrected for thickness and Poisson Ratio ($\nu = 0.5$) effects for comparison with Bowie's solution.

2) Cracks Parallel to the Bondline

These results (Table II) show that the values of K/K_0 were greater for cracks which were further from the bondline than those with smaller separate distance from there, suggesting the presence of a shielding effect due to the bondline. The variation of K/K_0 with a/w for both square and half height specimens are shown in Fig. 7. Also shown is a solution (Bowie and Neal, 1965) for homogeneous square specimens for both uniform displacement and uniform stress.

The larger gradients in the experimental curves above the theoretical results are conjectured to be partly due to slippage in the grips which tended to achieve more of a uniform load effect and partly due to the effect of the bondline. The experimental data suggests that both the shorter cracks and those closer to the bondline may have benefited from a shielding effect due to the higher bondline modulus.

It was also found that, in analyzing the data for the cracks in the half height specimen, a modification of the form of the non-singular stress between the crack and the bondline as described in Smith, Finlayson, and Liu, (1998) was necessary. This is believed due to a residual stress field very close to the bondline. A second half height specimen did not show bondline residual stress and was analyzed as described in the Appendix. Results were virtually identical with the results for the specimen with residual stress.

In assessing the overall effect of these residual stresses, it was found that while the SIF values above and below the crack tip in the square specimens differed by about 2%, those in the half height specimens differed by 6%. These differences were minimized by averaging the results in Table II.

In summary, results show that:

1) Normalized SIFs increase with relative crack length for both square and half height bonded specimens more rapidly than indicated by solutions for unbonded specimens for both bondline cracks and cracks parallel to the bondline.

2) Reducing specimen height reduces normalized SIF's for all crack lengths in both bondline cracked specimens and those containing cracks parallel to the bondline. Since Torvik, (1979) indicated such an effect in unbonded edge cracked specimens, this reduction appears to be due to specimen shape rather than a bondline effect and may be conjectured to apply to the bondline cracked specimen results as well.

4

3) The experiments revealed

   a) No shear mode effect

   b) A shielding effect due to the bondline for short cracks and those with less separation from the bondline for the cracks parallel to the bondlines.

4) Imperfections in the glued tab arrangement were clearly shown.

ACKNOWLEDGMENTS

REFERENCES

Bowie, O. L., "Symmetric Edge Cracks in Tensile Sheet with Constrained Ends," *Journal of Applied Mechanics*, pp. 726-728, Dec. (1964).

Gross, B., Srawley, J. E., and Brown, W. F., "Stress Intensity Factors for a Single-Edge Notch Tensile Specimen by Boundary Collocation of a Stress Function." *Technical Note D-2395 NASA*, 11 pages, Aug. (1964).

Bowie, O. L., and Neal, D. U., "Stress Intensity Factors for Single Edge Cracks with Constrained Ends," AMRA-TR 65-20, (1965).

Torvik, P. J., "On the Determination of Stresses, Displacements, and Stress Intensity Factors in Edge Cracked Sheets with Mixed Boundary Conditions," *Trans. ASME Series E. J. Ap. Mech.*, Vol. 46, pp. 611-617, (1979).

Hutchinson, J. W., and Suo, H., "Mixed Mode Cracking in Layered Materials," *Advances in Applied Mechanics*, Vol. 29, New York, Academic Press, pp. 63-91, (1992).

Smith, C. W., and Kobayaski, A. S., "Experimental Fracture Mechanics," Chapter 20: *Handbook on Experimental Mechanics*, 2nd Ed., Kobayashi, A. S., Ed. VCH New York, pp. 905-968, (1993).

Smith, C. W., Finlayson, E. F., and Liu, C. T., "Influence of Material Properties on SIF's Determined by Frozen Stress," *Journal of Engineering Fracture Mechanics*, Vol. 61, No. 5/6, pp. 555-568, (1998).

APPENDIX

Beginning with the Griffith-Irwin Equations, we may write, for Mode I, for the homogeneous case

$$\sigma_{ij} = \frac{K_1}{(2\pi r)^{1/2}} f_{ij}(\theta) + \sigma_{ij}^o \quad (i.j. = n, z) \qquad (1)$$

where: σ_{ij} are components of stress, K_1 is SIF, r, θ are measured from crack tip (Fig. A-1), σ_{ij}^o are non-singular stress components.

Then, along $\theta = \pi/2$, after truncating σ_{ij}

$$(\tau_{nz})_{max} = \frac{K_1}{(8\pi r)^{1/2}} + \tau^o = \frac{K_{AP}}{(8\pi r)^{1/2}} \qquad (2)$$

where $\tau^o = f(\sigma_{ij}^o)$ and is constant over the data range, K_{AP} = apparent SIF, $(\tau_{nz})_{max}$ = maximum shear stress in nz plane

$$\therefore \frac{K_{AP}}{\bar{\sigma}(\pi a)^{1/2}} = \frac{K_1}{\bar{\sigma}(\pi a)^{1/2}} + \frac{\sqrt{8}\tau^o}{\bar{\sigma}} \left(\frac{r}{a}\right)^{1/2} \qquad (3)$$

where (Fig. A-1) a = crack length, and $\bar{\sigma}$ = remote normal stress i.e.

$$\frac{K_{AP}}{\bar{\sigma}(\pi a)^{1/2}} \text{ vs. } \sqrt{\frac{r}{a}} \text{ is linear}$$

Since from the Stress-Optic Law $(\tau_{nz})_{max} = nf/2t$ where, n = stress fringe order, f = material fringe value, t = specimen thickness, then from Eq. 2, $K_{AP} = (8\pi r)^{1/2}(\tau_{nz})_{max} = (8\pi r)^{1/2} nf/2t$. A typical plot of normalized K_{AP} vs. $\sqrt{r/a}$ for a homogeneous specimen is shown in Fig. A-2.
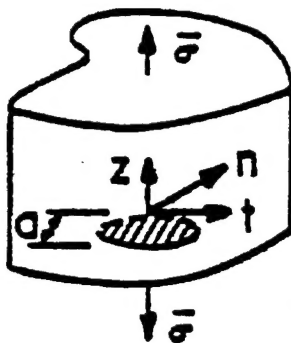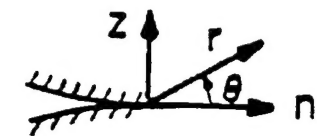
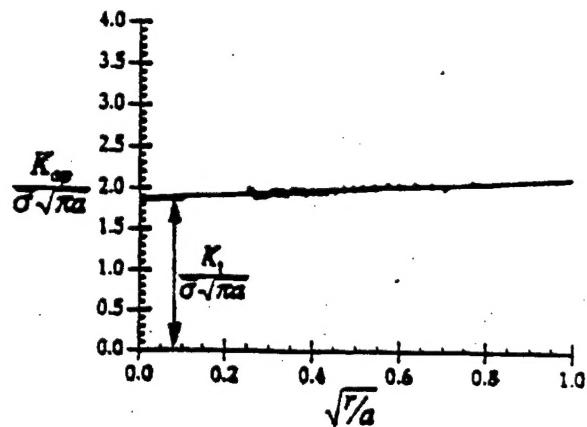Figure A-1: Mode I Near-Tip
Notation

Figure A-2 – Estimating Normalized
SIF from Test Data

Table 1 - Data and Results for Cracks Within Bondline

test#	a(mm)	h(mm)	a/b	P (N)	exp K/Ko	exp. corr. ($\nu = 0.5$) K/Ko	Bowie* ($\nu = 0.3$) K/Ko
DS2	7.94	50.8	0.16	74.95	1.14	1.05	1.06
DS3	12.7	50.8	0.25	74.95	1.09	1.00	1.04
DS4	17.4	50.8	0.34	74.95	1.15	1.06	1.04
DS5	20.6	50.8	0.41	74.95	1.23	1.13	1.06
DS6	25.4	50.8	0.50	74.95	1.38	1.27	1.10
DS7	27.9	50.8	0.55	74.95	1.37	1.26	1.12
DS8	7.94	25.4	0.16	74.95	0.93	0.86	—
DS9	12.7	25.4	0.25	74.95	0.94	0.87	—
DS10	17.4	25.4	0.34	52.68	0.98	0.90	—
DS11	20.6	25.4	0.41	50.72	1.00	0.93	—
DS12	25.4	25.4	0.50	50.72	1.18	1.09	—
DS13	27.9	25.4	0.55	51.01	1.22	1.12	—

* plane stress, no bondline $K_0 = \bar{\sigma}\sqrt{\pi a}$

Table 2 - Data and Results for Cracks Parallel to Bondline

w = 101.6

Test #	a	d	h	a/w	K^*/K_0
SP6	2.78	2.58	50.80	0.027	0.976
SP7	2.98	1.19	50.80	0.029	0.885
SP8	8.33	2.58	50.80	0.082	1.139
SP9	7.95	1.19	50.80	0.078	1.017
SP10	13.09	1.19	50.80	0.129	1.173
SP11	12.70	2.58	50.80	0.125	1.365
SP12	2.58	2.78	25.4	0.025	0.806
SP13	7.54	2.78	25.4	0.074	0.876
SP14	12.70	2.78	25.4	0.125	1.028

Dimensions in mm, * Corrected for 3-D effects to a 2D solution.
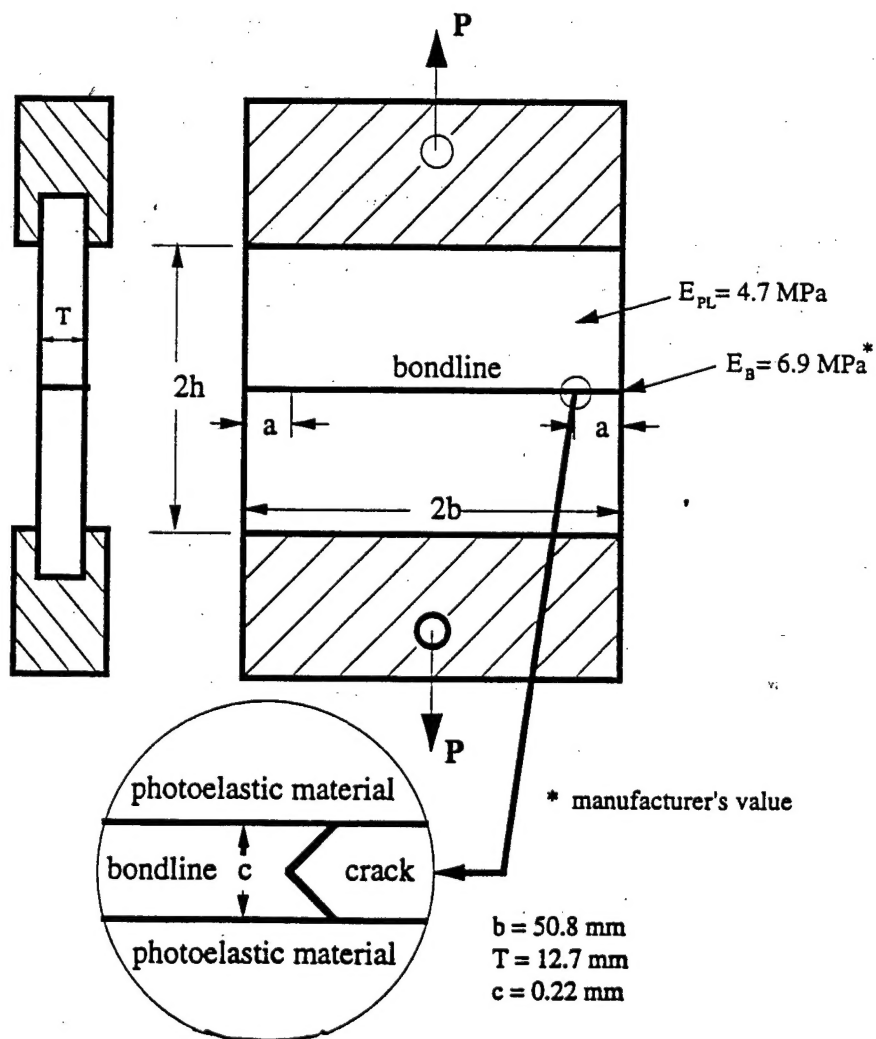
Figure 1 Bondline Specimens with Double Edge Bondline Cracks
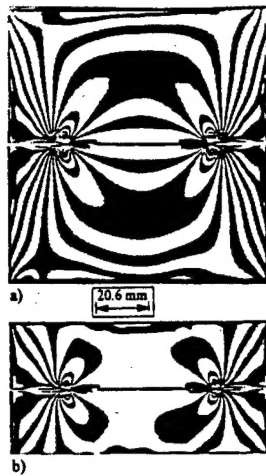
Figure 2: Global Stress Fringe Patterns for Bondline Crack in a) square b) short specimens (Integral Fringes white).

$P_1 + P_2 = 110.55$ N
$T = 12.70$ mm
$t = 0.23$ mm
$w = 101.6$ mm
$h = 50.8$ mm or 25.4 mm
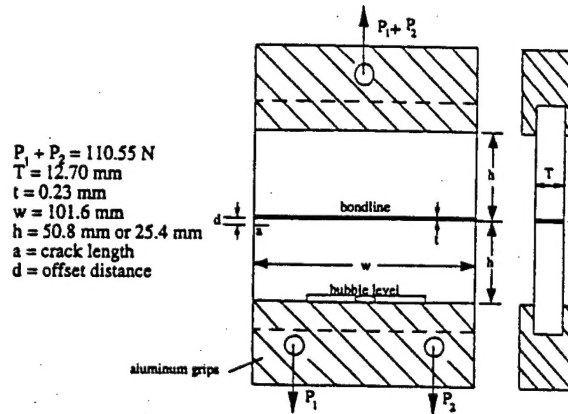a = crack length
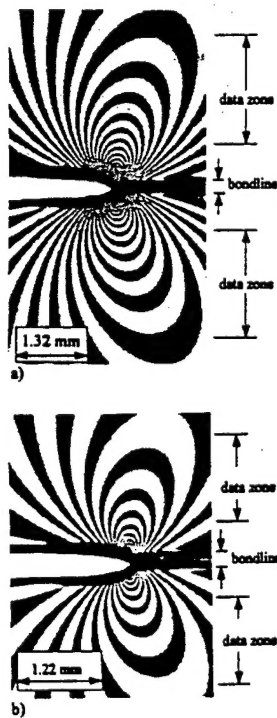d = offset distance

Figure 4: Test specimen and End Tabs; Crack Parallel to Bondline.

Figure 3: Local Stress Fringe Patterns for Bondline Cracks in a) square b) short specimens (Integral Fringes White).
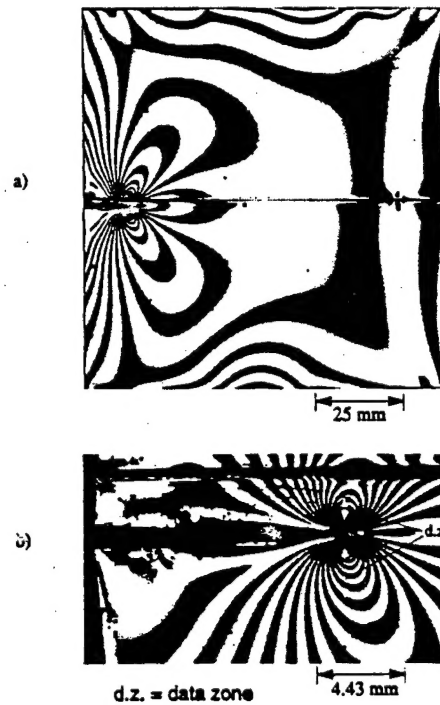

d.z. = data zone

Figure 5: a) Global and b) Local Stress Fringe Photos for Square Specimen with Crack Parallel to Bondline (Integral Fringes are Dark)
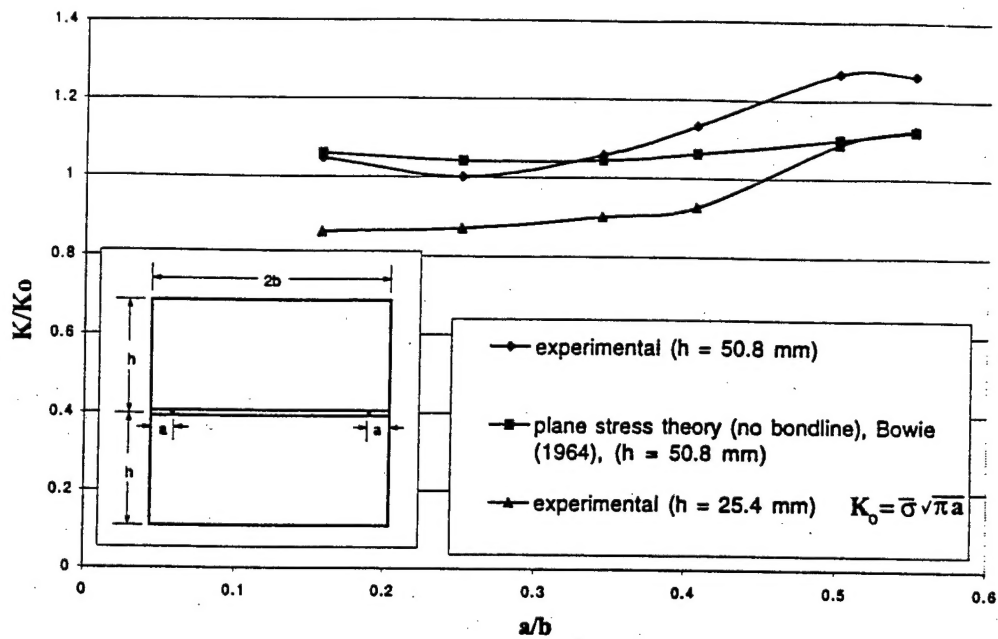
Figure 6 Normalized SIF vs. Normalized Crack Length for
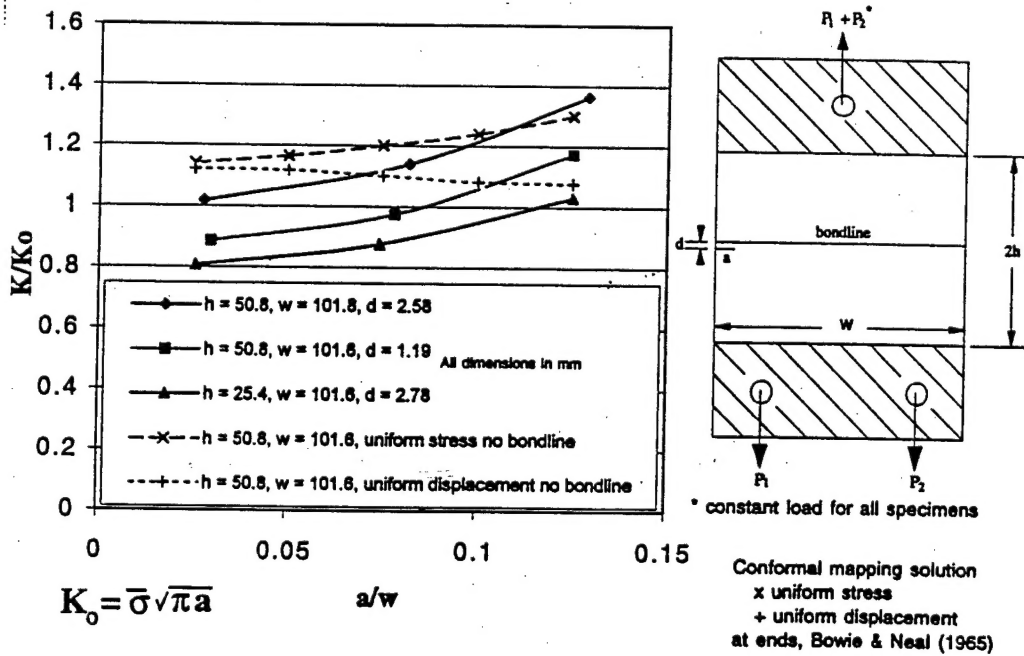Bondline Cracks (b = 50.8mm).

Figure 7 Normalized SIF vs. Normalized Crack Length for
Cracks Parallel to Bondline.